# DenserNet: Weakly Supervised Visual Localization Using Multi-scale Feature Aggregation

Dongfang Liu\*, Yiming Cui\*, Liqi Yan, Christos Mousas, Baijian Yang, Yingjie Chen

Abstract—In this work, we introduce a Denser Feature Network (DenserNet) for visual localization. Our work provides three principal contributions. First, we develop a convolutional neural network (CNN) architecture which aggregates feature maps at different semantic levels for image representations. Using denser feature maps, our method can produce more keypoint features and increase image retrieval accuracy. Second, our model is trained end-to-end without pixel-level annotation other than positive and negative GPS-tagged image pairs. We use a weakly supervised triplet ranking loss to learn discriminative features and encourage keypoint feature repeatability for image representation. Finally, our method is computationally efficient as our architecture has shared features and parameters during computation. Our method can perform accurate large-scale localization under challenging conditions while remaining the computational constraint. Extensive experiment results indicate that our method sets a new state-ofthe-art on four challenging large-scale localization benchmarks and three image retrieval benchmarks.

# I. INTRODUCTION

The task of visual localization is to predict the geographic location of a query image, based on its comparisons to GPS-tagged images from a database [1], [2], [3]. Visual localization has drawn considerable attention recently due to its potential value to the wide-ranging applications such as in robot navigation or autonomous driving [4], [5], [6], [7], [8]. Under the region where GPS signal is partially or completely shadowed, visual localization is an effective addition to GPS to support the operation of these mobile agents.

In our work, we cast the visual localization problem as an image retrieval task [9], [10]. Image retrieval task relies on local features to search over a GPS-tagged image database to estimate the current location. The primary challenge is how to produce discriminative image representation so that images from nearby locations would have similar representations while images from different locations would have dissimilar representations. Typically, a large-scale database contains images of similar man-made structures or landmarks that may cause severe ambiguities. Illumination changes or occlusions may also change object appearances which compromises the localization prediction [11]. To address these problems, our method is designed to be robust for a large-scale dataset with different challenging conditions (Figure 1).

In the last decade, convolutional neural networks (CNNs)

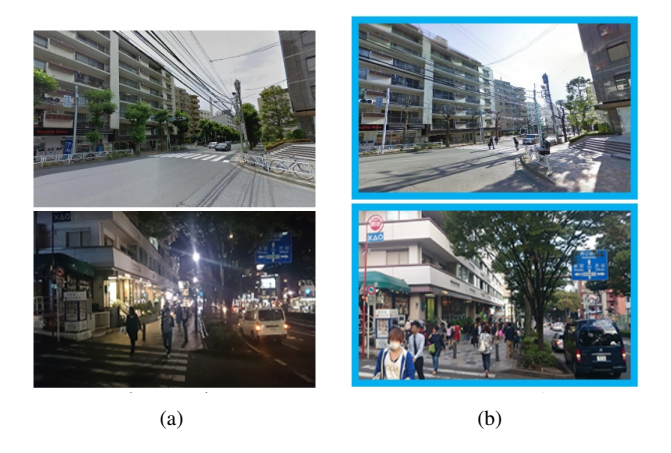


Fig. 1. DenserNet can correctly perform visual localization under challenging conditions. Despite environmental variations (such as pedestrian or vehicle occlusions, illumination changes, and seasonal changes), DenserNet can find the location (a) from the database based on the query (b).

have emerged as powerful technique to explore image representations including visual localization [3], [2], [12], [13], [14], [15], [16]. CNN-based visual localization networks have a similar architecture [17], [18]. They generally have a convolutional backbone encoder to produce feature maps of the input image. Then, a detection-description decoder organizes the obtained feature maps to depict the image representation [19], [20]. The conventional approaches only use the feature maps from a single semantic level and fail to exploit multi-scale features from different semantic levels. This limitation motivates our approach to exploit features from multi-level semantics to improve the performance of the visual localization.

So far, many state-of-the-art methods are trained using pixel-level annotations to supervise the process of feature learning [17], [21], [22]. However, the ground truth correspondences between image pairs are expensive to obtain at the scale required to train a CNN-based method. Also, such supervised priors based on human annotations may not fully capture all relevant features for image representation to train a network [18]. Thus, training a CNN-based method with strong supervision is not efficient and effective enough for generalization. In contrast, an increasing number of studies [9], [18] employ a weakly supervised manner for training using image-level labels. They compute the feature distance between the query-positive and the query-negative image pairs to discovery imagery discriminativeness. These prior

<sup>\*</sup> authors equally contributed to this work.

D. Liu, C. Mousas, B. Yang and Y. Chen are with Purdue University.

Y. Cui is with University of Florida.

L. Yan is with Fudan University.

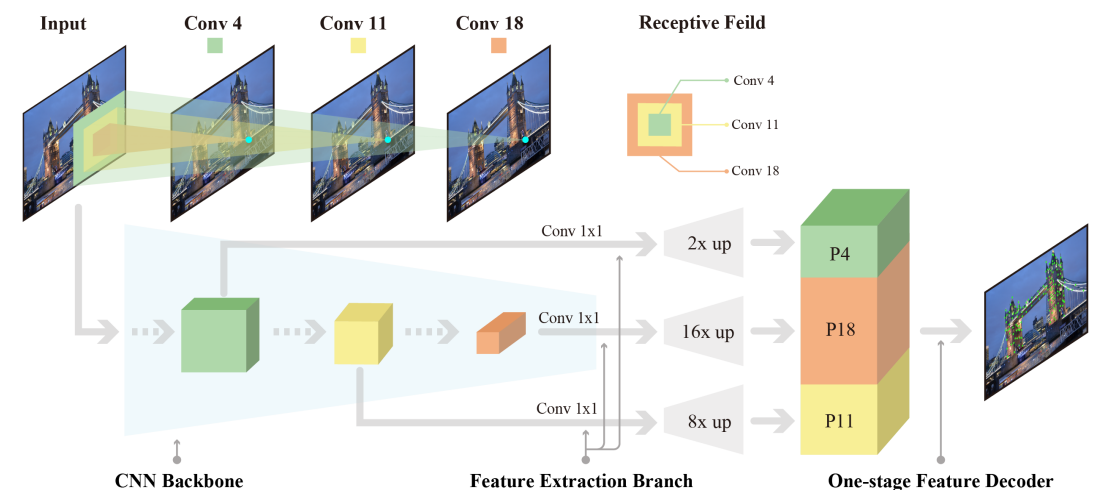


Fig. 2. The demonstration of DenserNet using MobileNet backbone [12]. The proposed method can aggregate multi-level feature maps and thus produce significantly more local keypoint features than concurrent methods [9], [17]. For simplicity,  $3 \times 3$  convolution layers after upsampling are not shown.

explorations impact our work.

Building on the lessons learnt from the concurrent approaches [9], [23], our work brings the following three contributions. First, we introduce a Denser Feature Network (DenserNet), a novel CNN-based method for visual localization task. We find inspiration from DenseNet [24] to aggregate feature maps at different semantic levels for image representations, as shown in Figure 2. Our method is an intuitive extension of NetVLAD [9] by adding feature extraction branches to obtain multi-scale features, in parallel with the existing backbone network. The feature extraction branches aggregate features from the lower-level, the mid-level, and the higher-level layer of the backbone network. Compared to conventional methods [17], [18], [23], our approach is able to produce denser keypoint features which increase the number of inlier matches between image pairs and, in turn, improve the matching accuracy under challenging conditions. Extensive experiment results indicate that our method improves the visual localization performance on several benchmarks by a large margin.

Second, we propose a weakly supervised approach for training. We design a modified triplet ranking loss to effectively organize obtained features and predict image representations. Our training requires no expensive pixel-wise ground truths other than GPS-tagged images, which are easy to obtain. In our design, task-relevant keypoint features are discovered in an unsupervised fashion, as the proposed method is able to learn in which context should be suppressed or emphasized to achieve a better location recognition. Inspired by [17], our training method performs a joint optimization for both detection and description tasks, which encourages the repeatability of discriminative detection and improves the description accuracy.

Finally, DenserNet is computationally efficient. Since the three feature extraction branches are all based on the same CNN backbone, they have shared features and parameters during computation. Theoretical and empirical evaluations demonstrate that, although DenserNet uses extra sub-network

branches to aggregate more feature maps for the location inference, it only requires a limited additional computation load. Thus, our method can achieve an efficient inference and remain within the computational constraints.

#### II. RELATED WORK

Recent advances in CNNs have made it possible to use local keypoint features of an image to predict location hypothesis [9]. Although the CNN-based approaches are proved to be effective for visual localization, they struggle to perform well when the feature homogeneousness occurs substantially [25]. Modern man-made structures frequently have architectural similarities so it is difficult for the conventional methods to handle this challenging situation [1]. In addition, the performance of conventional methods typically degrades under extreme environmental changes, such as illumination or landmark scale changes [17].

A critical reason causing these problems for conventional methods [9], [18] is that they only use features from one semantic level for the final prediction. Thus, they fail to exploit features from different levels of semantics to capture more multi-scale details. This semantic gap introduces a critical problem in both feature learning and predicting [26]. To address the above challenges, our method is designed to produce more keypoint features using feature extraction branches from different semantic levels. Since our feature extraction branches are paralleled to the backbone network, the proposed method is computationally efficient for features sharing. We aggregate features with both strong semantics and high spatial resolution to obtain discriminative representation. Thus our method is robust to environmental changes such as illumination and landmark scale changes.

#### III. DENSERNET

## A. Overview

The architecture of DenserNet is shown in Figure 2. DenserNet includes a CNN backbone, three feature extraction branches, and an one-stage feature decoder. Our design

leverages the intrinsic nature of modern CNN architecture which can produce rich hierarchical features from different convolutional layers from a single forward pass. Thus we can obtain multi-scale features with low additional costs to close the semantic gap in feature learning. Each feature extraction branch sticks out at different layers of the backbone network to extract features from different semantic levels. We aggregate the obtained features to capture strong image representation. Intuitively, our method is more robust to scale variances than methods learned from single-scale features and thus improves the localization performance. We elaborate the detail of our method below.

#### B. Feature Extraction Branch

The design of DenserNet is flexible and allows various backbone options. For fast runtime, we use MobileNetV2 [12], a light-weighted network, as our backbone network. DenserNet has the lower-level, the mid-level, and the higher-level branch as they branch out at different locations of the backbone. Specifically, the lower-level and mid-level branches stick out at the conv4 and conv11 respectively, and the higher-level branch is attached to the conv18.

The input features for each feature extraction branch are  $\{C4, C11, C18\}$ , having strides of  $\{4, 16, 32\}$  pixels with respect to the input image. Each feature extraction branch employs a modified SuperPoint layer [23]. Instead of having the keypoints and local descriptors from the original implementation, the modified SuperPoint only increases the channel dimensions and upsamples the feature maps. The SuperPoint layer has a shallow structure of a non-linear  $1 \times 1$ convolutional layer and a upsampling layer. The non-linear  $1 \times 1$  convolutional layer with ReLU6 activation is used to increase the channel dimensions of each branch. The upsampling layer increases the spatial resolution of the feature maps in a non-learned manner, which is much faster than using transposed convolutions [26]. After SuperPoint layer, the output feature maps are  $\{P4, P11, P18\}$  corresponding to  $\{C4, C11, C18\}$ . Compared to  $\{C4, C11, C18\}$ , the channel dimensions for  $\{P4, P11, P18\}$  increase 3, 1.5, 1.1 times respectively and their spatial resolutions is brought back to the half of the input resolution, which supports more tentative keypoint predictions. Following the practice from [27], we also append a  $3 \times 3$  convolution on each output in order to reduce the aliasing effect from upsampling. The obtained features from each feature extraction branch are aggregated by channel-wise concatenation. The aggregated features are dense with channel dimensions of 520. Then, we use onestage feature decoder to produce image representation, which is discussed in the next section.

The core concept for our design is to leverage the dense features to enhance image representations. Following the simple rule, our approach can use many design choices. Adding more feature extraction branches (more than three) can improve the prediction performance but demand more memory footprint. Empirically, our method has the best runtime and accuracy tradeoff. We also implement a VGG16 [13] version of DenserNet. More details of our method

architecture are provided in the appendix.

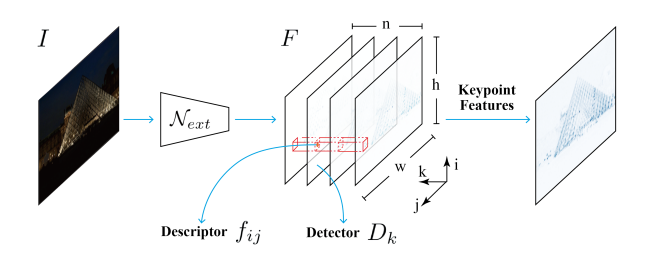


Fig. 3. One-stage feature decoder. We couple descriptor and detector together to extract keypoint local features.

# C. One-stage Feature Decoder

Similarly to [17], we employ one-stage feature decodor in DenserNet which couples detectors and descriptors closely as shown in Figure 3. The feature extraction branches and the backbone network together work as the feature extraction encoder  $\mathcal{N}_{ext}$  that processes the input image I and produces the dense feature maps  $F = \mathcal{N}_{ext}(I)$ ,  $F \in \mathbb{R}^{h \times w \times n}$  (where  $h \times w$  is the feature map size and n is the number of channels). The one-stage feature decoder performs detection and description simultaneously to prevent information loss in the quantization step.

**Feature descriptor.** The feature maps F can be expressed by a set of descriptor vectors f:

$$f_{ij} = F_{ij:}, f_{ij} \in \mathbb{R}^n, \tag{1}$$

where  $i \in \mathbb{R}^h$  and  $j \in \mathbb{R}^w$ . These descriptor vectors can be used to establish feature correspondences by calculating the Euclidean distance between images. We use L2 normalization to make the obtained descriptors in unit length. Then, we properly adjust these descriptors in training so that the same points for a scene produce similar descriptors, which robustly describe discriminative appearance variations.

**Feature detector.** In the same vein, the feature maps F can be expressed as a collection of detector D:

$$D_k = F_{::k}, \quad D_k \in \mathbb{R}^{h \times w} \tag{2}$$

where  $k \in \mathbb{R}^n$ . In this expression, the feature extraction network  $\mathcal{N}_{ext}$  produces n different detection response maps  $D_k$ . If pixel point (i,j) is detected, we denote a hard feature detector  $D_{(ij)k}$  which is the most strong detection in all channels. We then perform a channel-wise softmax around its neighbours to obtain the local softmax score:

$$\alpha_{ij} = \frac{\exp(D_{(ij)k})}{\sum_{i'=i-1}^{i+1} \sum_{j'=j-1}^{j+1} \exp(D_{(i'j')k})}.$$
 (3)

Finally, we compute an image-level normalization for the softmax score and obtain the detection score at a pixel (i, j):

$$s_{ij} = \frac{\alpha_{ij}}{\sum_{i'=1}^{h} \sum_{j'=1}^{w} \alpha_{i'j'}}.$$
 (4)

#### D. Time Complexity Analysis

Similar to the conventional methods [9], [23], our method has a backbone encoder for feature extraction and feature decoder for image representation. However, our approach also includes three feature extraction branches stick out from the lower, middle, higher level of the backbone network to efficiently produce denser features. Unlike patch-based networks MNV [28] and LF-Net [21] who adopt a Siamese sub-network to produce more features with a high computational cost, our approach has shared features across the three branches, which require limited extra computation.

For runtime complexity, the ratio of our approach versus the conventional methods is:

$$r = \frac{\mathcal{O}(\mathcal{N}_{cnn}) + 3 \times \mathcal{O}(\mathcal{N}_{br}) + \mathcal{O}(\mathcal{N}_{de})}{\mathcal{O}(\mathcal{N}_{cnn}) + \mathcal{O}(\mathcal{N}_{de})}.$$
 (5)

where  $\mathcal{O}(\mathcal{N}_{cnn})$ ,  $\mathcal{O}(\mathcal{N}_{br})$ , and  $\mathcal{O}(\mathcal{N}_{de})$  are the function complexity for the backbone encoder, the feature extraction branch, and the feature decoder for image representation. Since  $\mathcal{O}(\mathcal{N}_{de}) \ll \mathcal{O}(\mathcal{N}_{cnn})$ , the ratio can be approximated as:  $r \approx 1 + \frac{3 \times \mathcal{O}(\mathcal{N}_{br})}{\mathcal{O}(\mathcal{N}_{cnn})}$ . Compared to the conventional methods, the increased computational cost of the proposed method mainly comes from  $\mathcal{N}_{br}$  branches. This increased computational cost can be ignored because  $\mathcal{O}(\mathcal{N}_{br}) \ll \mathcal{O}(\mathcal{N}_{cnn})$ . Thus, our approach is appealing for its efficiency. More detailed reports are displayed in the results section.

#### E. Training Objective

We propose a modified triplet ranking loss to jointly optimize our detectors and descriptors in a weakly supervised manner, which only requires cheap image triplets for training. In our setting, the location of a query image  $I_q$  is approximated by searching for the nearest neighbors in feature space among the reference images  $\{I_r\}$ . Thus, the objective for training our method is to match the positive references  $\{I_r^+\}$  which are closer to the query image and vice-versa to the negative ones  $\{I_r^-\}$ .

For a pair of images  $(I^1,I^2)$  and potential corresponding feature points  $P:p_1\leftrightarrow p_2$  between them (where  $p_1\in I^1,p_2\in I^2$ ), we want to minimize the distance  $\sum_{p\in\mathcal{P}}\parallel f_p^1-f_p^2\parallel_2$  of the corresponding descriptors between the positive pairs while maximize the distance between the negative ones. In order to increase the repeatability of detection [17], we also add a detection term to encourage repeatability of effective detection between two images:

$$\mathcal{R}\left(I^{1}, I^{2}\right) = \sum_{p \in P} \frac{s_{p}^{1} s_{p}^{2}}{\sum_{p' \in P} s_{p'}^{1} s_{p'}^{2}} \parallel f_{p}^{1} - f_{p}^{2} \parallel_{2}.$$
 (6)

where P is the set of all corresponding feature points between  $I^1$  and  $I^2$ .  $s_p^1$  and  $s_p^2$  are the detection scores in (4) at each corresponding feature point of the paired images. Accordingly, our training objective can be defined as:

$$\mathcal{L}_{\mathcal{R}}\left(I_{t}, I_{r}^{+}, I_{r}^{-}\right) = \max\left(M + \mathcal{R}\left(I_{t}, I_{r}^{+}\right) - \mathcal{R}\left(I_{t}, I_{r}^{-}\right), 0\right). \tag{7}$$

where  $I_t$ ,  $I_r^+$ , and  $I_r^-$  are the training query image, the positive reference, and the negative reference respectively. In order to minimize the proposed loss, the distances of the discriminative descriptors between the training query and the positive reference are encouraged to be small and the associated detection scores are enforced to be large. Using the weakly supervised fashion for training, our method effectively learns feature representation pertaining to which features should be suppressed or emphasized.

#### IV. EXPERIMENTS AND RESULTS

In this section, we first describe the implementation details and the evaluation datasets. We then use ablation study to investigate the improvements of our method from the baseline method. Next, we test the proposed method on several tasks in comparison with some of the state-of-the-art methods. Finally, we conclude with the runtime evaluation.

## A. Implementation Details

**Training data.** Google Street View Time Machine (GSVTM) datasets have been widely-used in training weakly supervised methods for visual localization [29], [25]. GSVTM includes image data of a same location multiple times under different illuminations or seasons. These environmental variations provide the learning algorithm rich information about what features should be learned, in order to achieve a robustness in prediction. Each image is labelled with a GPS tag so we can use the geo-location information to identify nearby images.

Specifically, we train the proposed method by using Pitts30k-training dataset [9]. Following [9], [18], we group the positive  $\{I_r^+\}$  and negative  $\{I_r^-\}$  images for each training query image  $I_t$ . The positive image is the closest neighbor to each query image in the feature embedding space at its nearby geo-locations, while the negative image are far away ones. The 30K training query images generate four image triplets. Thus, we obtain a total of 120K image triplets with 112K for training and 8K for validation.

**Training process.** Our training and evaluation are performed on a workstation with an Intel Core i7-7820X CPU and one NVIDIA GeForce GTX 1080Ti GPU. We implement both VGG16 and MobileNetV2 based methods, which are pretrained on ImageNet [30]. For the MobileNet-based method, 30 epochs are performed using batch size of 4 triplets, Adam [31] with the learning rates of  $10^{-3}$  which is halved every 6 epochs, momentum of 0.9, and weight decay of  $10^{-3}$ . This implementation allow us to achieve desired training results but convergence generally occurs faster than the designated training length. We use the Precision-Recall curve to evaluate the training performance [9]. A query is considered to be correct if at least one result from the top Nretrieved database images is within d = 25 meters from the ground truth position of the query image. We use the best method (the highest recall@5) on the validation for testing. More training details about the VGG-based method can be found in the appendix.

#### B. Evaluation Datasets and Metrics

We assess our method on three different tasks with a number of publicly available benchmarks.

**Feature matching task.** HPatches dataset [32] is adopted to evaluate the effectiveness of feature extraction and matching. To evaluate detector, we examine the detection repeatability and mean localization error (MLE) of the keypoint features which determine the matching reliability and the number of inlier matches. To evaluate descriptor, we compute the mean average precision (mAP) and the matching score (MS). The mAP assesses a method's ability to suppress spurious matches. MS reflects the overall performance of both detector and the descriptor.

Large-scale visual localization task. Pitts 250k-test [33], Tokyo 24/7 [29], Tokyo TM-val [9], and and Sf-0 [34] are used to investigate the performance of visual localization. For the first three benchmarks, a query is considered to be correct if at least one result from the top N retrieved database images is within d=25 meters from the ground truth position of the query image. For Sf-0, the query result is considered to be correct if at least one result from the top N retrieved database images has a same building ID.

**Image retrieval task.** Since we cast the visual localization problem as an image retrieval task, we also evaluate our method on image retrieval benchmarks. Oxford 5k [35], Holidays [36] and Paris 6k [37] are used to test the generalization of our method for image representations on image retrieval. We use mAP for evaluation.

Method	НВ	LB	МВ	Detecto	r Metric	Descriptor Metric		
Wichiou				Rep.	MLE	mAP	MS	
a(M) b(M) c(M) d(M)		<b>√</b>		0.556 0.568 0.573 0.592	0.99 1.02 1.03 1.04	0.782 0.799 0.808 0.827	0.448 0.456 0.461 0.473	
a(V) b(V) c(V) d(V)		√   √	\  \  \  \  \	0.578 0.588 0.596 0.628	1.12 1.14 1.15 1.17	0.822 0.847 0.859 0.886	0.462 0.471 0.475 0.481	

TABLE I. Evaluation results from HPatches dataset. We use HPatches to examine the ability for feature extraction and matching. Method a is the baseline while method b and c are its variants. Method d is the proposed DenserNet. The results indicate the improvements of DenserNet from baseline in the all metrics. M and V in methods stand for MobileNet and VGG-based backbones respectively. HB, LB, MB stand for higher-level, lower-level, and mid-level branch respectively.

# C. Ablation Study

We conduct an ablation study to validate the improvements of DenserNet from a strong baseline and its variants. Method (a) is the baseline which only has the higher-level branch for feature extraction. It is identical to SuperPoint [23]. Method (b) and (c) are two variants of the baseline method with the additional lower-level or mid-level branch respectively. Method (d) is the proposed method. The ablation study is conducted on feature matching and visual localization tasks.

The results for feature matching are demonstrated in Table I. As expected, VGG-based methods outperform their MobileNet-based counterparts because VGG16 has the better feature extraction capacity. From method (a) to method (d), adding the feature branch can give a boost in the performance of both detector and descriptor. The repeatability of keypoint features increases with the increase of the feature extraction branch while errors only increase with a small scale. Meanwhile, mAP and matching scores also increase accordingly by adding the feature extraction branch. Figure 4 demonstrates the qualitative results of the VGG-based method. Our method can produce more keypoint features for effective matching than the baseline method.

The results for large-scale visual localization tasks are demonstrated in Figure 5. Method (d) outperforms the baseline method and its variants on all benchmarks. We observe a steady increase of recall@N from method (a) to method (d). Based on the Precision-Recall curve, using extra feature extraction branch is proved to be effective to improve the performance of localization as methods having more feature extraction branches achieve better results on all benchmarks. More results for both tasks are provided in the appendix.

## D. Comparison with State-of-the-Art Methods

To demonstrate the advancement of the proposed method, we compare our method with the state-of-the-art methods on large-scale localization benchmarks and image retrieval tasks. We choose three leading methods NetVLAD, CRN, and SuperPoint for comparison. In order to have a fair comparison, we retrain all the methods with the same setup.

Large-scale localization benchmark results. We report the recall@N results for different methods in Table II. Both our VGG16 and MobileNet-based methods consistently outperform state-of-the-art methods by a significant margin on all benchmarks. For instance, on the Pitts250k dataset, our improvements over the next best method NetVLAD at r@1 is 3.45% for the VGG-based architecture and 1.87% for the MobileNet-based architecture. On the Sf-0 dataset, our VGG16 and MobileNet-based methods achieve r@1 of 80.08% and 79.12% respectively compared to the next best method CRN by a margin of 3.18% and 1.5% respectively. Our methods also obtain similar improvements on Tokyo 24/7 and Tokyo TM. The results from all benchmarks confirm our assumption for this proposed work: leveraging denser features from multiple semantic levels and using a right supervision for training, the proposed method can effectively learn discriminative yet compact image representations for visual localization. The Precision-Recall curve for each method is shown in the appendix.

For qualitative analysis, we visualize the regions of the input image which are emphasized for localization prediction (as shown in Figure 6). Particularly, we use the heatmaps [38] to highlight the feature emphasis of different regions on the input image. Based on the results, we observe that our method is superior to its counterparts in identifying more useful features for localization, despite the significant

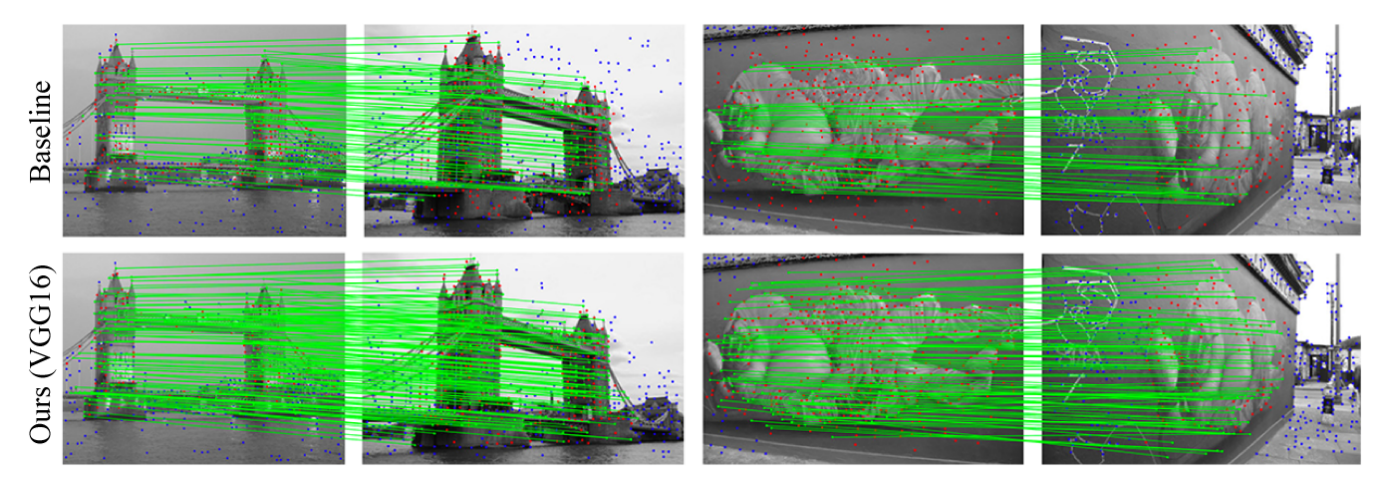


Fig. 4. Qualitative examples on the HPatches dataset. The green lines indicate all correct correspondences which are repeatable. DenserNet can produce denser and more correct matches compared to the baseline method. Red dots are mismatched points and blue dots are not visible to the shared viewpoint region of the image pairs.

Method	Pitts 250k-test		TokyoTM-val		Tokyo 24/7			Sf-0				
	r@1	r@5	r@10	r@1	r@5	r@10	r@1	r@5	r@10	r@1	r@5	r@10
Ours(VGG)	89.40	95.90	96.99	94.80	97.69	98.20	81.20	88.67	91.10	80.80	86.99	89.68
Ours(MobileNet)	87.82	94.89	96.26	94.62	97.37	98.12	79.17	87.99	90.17	79.12	85.68	88.56
CRN	85.50	93.49	95.50	93.07	95.97	97.61	75.39	83.81	87.31	77.62	84.31	86.80
NetVLAD	85.95	93.21	95.13	92.85	95.77	97.59	73.33	82.86	86.03	76.57	83.27	85.80
SuperPoint	85.78	93.36	95.26	92.81	96.04	97.53	75.37	83.44	86.73	75.52	84.01	86.60

TABLE II. Comparison of Recalls at N top retrievals of different methods on the four large-scale visual localization benchmarks.

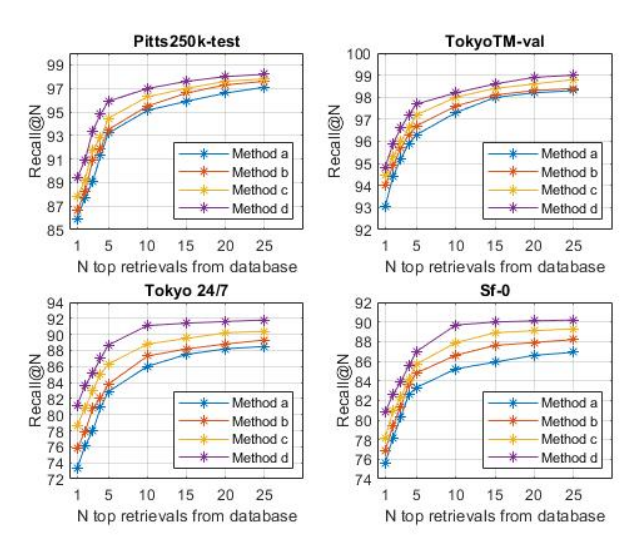


Fig. 5. Ablation results of Recalls at N top retrievals with all VGG-based methods.

environmental variations in viewpoint or illumination. Our method focuses on the distinctive details of buildings that are identifiable for visual localization while avoiding confusing visual clues. In contrast, other methods generally focus on local features independently which are inherently limited. Many features are laid on confusing scenes such as pedestrians, vegetation, or vehicles which are hard for feature repeatability. The results indicate that our method scales well to visual localization under large-scale environments. More

Method	Oxfo	rd 5k	Pari	s 6k	Holidays		
Wictiou	full	crop	full	crop	orig	rot	
Ours(VGG)	67.66	69.40	75.03	78.21	84.71	88.30	
Ours(MobileNet)	66.88	68.26	75.00	78.30	84.01	88.28	
CRN	63.95	65.52	72.88	75.85	83.19	87.30	
NetVLAD	63.09	65.33	72.53	75.67	82.67	86.83	
SuperPoint	63.14	65.50	72.83	75.10	82.92	86.90	

TABLE III. Comparison with state-of-the-art methods for compact image representations (256-D) on image retrieval tasks.

results are displayed in the appendix.

Image retrieval task results. To assess generalizability of our approach, we evaluate our methods trained only on Pitts30k [9] without any fine-tuning on the standard image retrieval datasets. For Oxford 5k [35] and Paris 6k [37], we use both the full and cropped images; for Holidays [36], we use original and rotated images. The results are displayed in Table III. Our results set the state-of-the-art for compact image representations (256-D) on all three datasets. On all metrics, our margin consistently over the mAP of other methods is 1-4%. For example, there are a 3.71% (our VGG-based method) and 2.93% (our MobileNet-based method) improvements on Oxford 5k (full) than the next best method; there are a 3.88% (our VGG-based method) and 2.74% (our MobileNet-based method) improvements on Oxford 5k (crop) than the next best method. Since our methods only see building-oriented images, our results can be further improved by fine-tuning using the natural landmark images from the three image retrieval datasets. Appendix

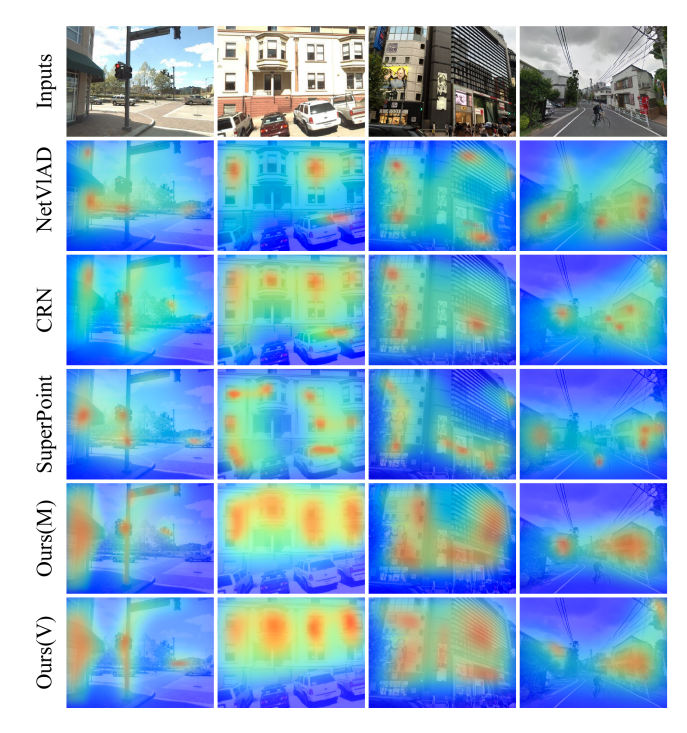


Fig. 6. Comparison of feature emphasis of each method. Our methods focus on the distinctive details of buildings which are identifiable for visual localization, while avoiding confusing visual clues such as pedestrians, vegetation, or vehicles which are hard for feature repeatability.

contains more results on varying the dimensionality of the image representation.

#### E. Runtime Evaluation

In design, our method is applicable to large-scale localization tasks in challenging conditions while remaining the computational constraint. We analyze its runtime and compare it with other state-of-the-art methods. All the measurements are conducted on the same work station. As shown in Table IV, the increase of our computation cost stems from feature extraction branch (FEB). However, this cost is affordable as it is much smaller than that of backbone encoderthe and thus it has little impact on the total runtime cost. Specifically, our MobileNet-based method is around 4× faster than CRN and NetVLAD which have the VGG-based architecture. For our VGG-based method, our speed is comparable to CRN and NetVLAD which have the same backbone network. Although our VGG-based methods are slower than SuperPoint which use a smaller backbone architecture, our methods outperform counterparts in localization r@1 by a large margin.

## V. CONCLUSION

In this work, we propose DenserNet, a novel CNN-based method that aggregates denser features to achieve strong image representation. Unlike conventional architectures which only use features from one semantic level, our method leverages multi-scale feature extraction branches to produce more keypoint features for image representation. Results from extensive experiments indicate that our method

Dataset	Method		r@1			
Dataset	Wichiod	BE	FEB	FD	Total	lei
•	Ours(V)	92	6	2	100	89.40
	Ours(M)	15	6	2	23	87.82
Pitts250k-test	CRN	92	-	6	98	85.50
	NetVLAD	92	-	5	97	85.95
	SuperPoint	43	-	7	50	85.78
	Ours(V)	96	7	3	106	81.20
	Ours(M)	18	7	3	28	79.17
Tokyo 24/7	CRN	96	-	8	104	75.39
	NetVLAD	96	-	7	103	73.33
	SuperPoint	49	-	9	58	75.37

TABLE IV. Runtime evaluation. BE, FEB, and FD means backbone encoder, feature extraction branch, and feature decoder respectively.

is competitive with the current state-of-the-art methods on large-scale localization tasks.

#### REFERENCES

- M. Salarian, N. Iliev, A. E. Cetin, and R. Ansari, "Improved image-based localization using sfm and modified coordinate system transfer," *IEEE Transactions on Multimedia*, vol. 20, no. 12, pp. 3298–3310, 2018
- [2] X. Li, S. Wang, Y. Zhao, J. Verbeek, and J. Kannala, "Hierarchical scene coordinate classification and regression for visual localization," 2020
- [3] B. Wang, C. Chen, C. X. Lu, P. Zhao, N. Trigoni, and A. Markham, "Atloc: Attention guided camera localization," 2019.
- [4] D. Liu, Y. Cui, Z. Cao, and Y. Chen, "A large-scale simulation dataset: Boost the detection accuracy for special weather conditions," in 2020 International Joint Conference on Neural Networks (IJCNN), 2020, pp. 1–8.
- [5] R. Mur-Artal, J. M. M. Montiel, and J. D. Tardos, "Orb-slam: a versatile and accurate monocular slam system," *IEEE transactions on robotics*, vol. 31, no. 5, pp. 1147–1163, 2015.
- [6] D. Liu, Y. Cui, Y. Chen, J. Zhang, and B. Fan, "Video object detection for autonomous driving: Motion-aid feature calibration," *Neurocomputing*, 2020.
- [7] D. Liu, Y. Cui, Z. Cao, and Y. Chen, "Indoor navigation for mobile agents: A multimodal vision fusion model," in 2020 International Joint Conference on Neural Networks (IJCNN), 2020, pp. 1–8.
- [8] A. F. Dalipi, D. Liu, X. Guo, Y. Chen, and C. Mousas, VR-PAVIB: The Virtual Reality Pedestrian-Autonomous Vehicle Interaction Benchmark. New York, NY, USA: Association for Computing Machinery, 2020, p. 38–41. [Online]. Available: https://doi.org/10.1145/3409251.3411718
- [9] R. Arandjelovic, P. Gronat, A. Torii, T. Pajdla, and J. Sivic, "Netvlad: Cnn architecture for weakly supervised place recognition," in *Proceedings of the IEEE conference on computer vision and pattern recognition*, 2016, pp. 5297–5307.
- [10] D. Liu, Y. Cui, X. Guo, W. Ding, B. Yang, and Y. Chen, "Visual localization for autonomous driving: Mapping the accurate location in the city maze," 2020.
- [11] G. Tolias, Y. Avrithis, and H. Jégou, "Image search with selective match kernels: aggregation across single and multiple images," *International Journal of Computer Vision*, vol. 116, no. 3, pp. 247–261, 2016.
- [12] M. Sandler, A. Howard, M. Zhu, A. Zhmoginov, and L.-C. Chen, "Mobilenetv2: Inverted residuals and linear bottlenecks," in *Proceedings of the IEEE conference on computer vision and pattern recognition*, 2018, pp. 4510–4520.
- [13] K. Simonyan and A. Zisserman, "Very deep convolutional networks for large-scale image recognition," arXiv preprint arXiv:1409.1556, 2014.
- [14] M. Zhang, W. Guo, Y. Cui, F. Shen, and Y. Shen, "Manifold learning based supervised hyperspectral data classification method using class encoding," in 2016 IEEE International Geoscience and Remote Sensing Symposium (IGARSS), 2016, pp. 3160–3163.
- [15] Z. Luo, L. Zhou, X. Bai, H. Chen, J. Zhang, Y. Yao, S. Li, T. Fang, and L. Quan, "Aslfeat: Learning local features of accurate shape and localization," 2020.

- [16] M. Zhang, Z. Lin, Y. Cui, F. Shen, and Y. Shen, "Multiclassification method for hyperspectral data based on chernoff distance and pairwise decision tree strategy," in 2016 IEEE International Geoscience and Remote Sensing Symposium (IGARSS), 2016, pp. 505–508.
- [17] M. Dusmanu, I. Rocco, T. Pajdla, M. Pollefeys, J. Sivic, A. Torii, and T. Sattler, "D2-net: A trainable cnn for joint detection and description of local features," arXiv preprint arXiv:1905.03561, 2019.
- [18] H. Jin Kim, E. Dunn, and J.-M. Frahm, "Learned contextual feature reweighting for image geo-localization," in *Proceedings of the IEEE Conference on Computer Vision and Pattern Recognition*, 2017, pp. 2136–2145.
- [19] J. Revaud, P. Weinzaepfel, C. D. Souza, N. Pion, G. Csurka, Y. Cabon, and M. Humenberger, "R2d2: Repeatable and reliable detector and descriptor," 2019.
- [20] M. Dusmanu, I. Rocco, T. Pajdla, M. Pollefeys, J. Sivic, A. Torii, and T. Sattler, "D2-net: A trainable cnn for joint detection and description of local features," 2019.
- [21] Y. Ono, E. Trulls, P. Fua, and K. M. Yi, "Lf-net: learning local features from images," in *Advances in neural information processing systems*, 2018, pp. 6234–6244.
- [22] J. L. Schonberger and J.-M. Frahm, "Structure-from-motion revisited," in *Proceedings of the IEEE Conference on Computer Vision and Pattern Recognition*, 2016, pp. 4104–4113.
- [23] D. DeTone, T. Malisiewicz, and A. Rabinovich, "Superpoint: Self-supervised interest point detection and description," in *Proceedings of the IEEE Conference on Computer Vision and Pattern Recognition Workshops*, 2018, pp. 224–236.
- [24] G. Huang, Z. Liu, L. Van Der Maaten, and K. Q. Weinberger, "Densely connected convolutional networks," in *Proceedings of the IEEE conference on computer vision and pattern recognition*, 2017, pp. 4700–4708.
- [25] L. Liu, H. Li, and Y. Dai, "Stochastic attraction-repulsion embedding for large scale image localization," in *Proceedings of the IEEE International Conference on Computer Vision*, 2019, pp. 2570–2579.
- [26] P.-E. Sarlin, C. Cadena, R. Siegwart, and M. Dymczyk, "From coarse to fine: Robust hierarchical localization at large scale," in *Proceedings* of the IEEE Conference on Computer Vision and Pattern Recognition, 2019, pp. 12716–12725.
- [27] T.-Y. Lin, P. Dollár, R. Girshick, K. He, B. Hariharan, and S. Belongie, "Feature pyramid networks for object detection," in *Proceedings of the IEEE conference on computer vision and pattern recognition*, 2017, pp. 2117–2125.
- [28] P.-E. Sarlin, F. Debraine, M. Dymczyk, R. Siegwart, and C. Cadena, "Leveraging deep visual descriptors for hierarchical efficient localization," arXiv preprint arXiv:1809.01019, 2018.
- [29] A. Torii, R. Arandjelovic, J. Sivic, M. Okutomi, and T. Pajdla, "24/7 place recognition by view synthesis," in *Proceedings of the IEEE Conference on Computer Vision and Pattern Recognition*, 2015, pp. 1808–1817.
- [30] J. Deng, W. Dong, R. Socher, L.-J. Li, K. Li, and L. Fei-Fei, "Imagenet: A large-scale hierarchical image database," in 2009 IEEE conference on computer vision and pattern recognition. Ieee, 2009, pp. 248–255.
- [31] D. P. Kingma and J. Ba, "Adam: A method for stochastic optimization," arXiv preprint arXiv:1412.6980, 2014.
- [32] V. Balntas, K. Lenc, A. Vedaldi, and K. Mikolajczyk, "Hpatches: A benchmark and evaluation of handcrafted and learned local descriptors," in *Proceedings of the IEEE Conference on Computer Vision and Pattern Recognition*, 2017, pp. 5173–5182.
- [33] A. Torii, J. Sivic, T. Pajdla, and M. Okutomi, "Visual place recognition with repetitive structures," in *Proceedings of the IEEE conference on* computer vision and pattern recognition, 2013, pp. 883–890.
- [34] D. M. Chen, G. Baatz, K. Köser, S. S. Tsai, R. Vedantham, T. Pylvänäinen, K. Roimela, X. Chen, J. Bach, M. Pollefeys et al., "City-scale landmark identification on mobile devices," in CVPR 2011. IEEE, 2011, pp. 737–744.
- [35] J. Philbin, O. Chum, M. Isard, J. Sivic, and A. Zisserman, "Object retrieval with large vocabularies and fast spatial matching," in 2007 IEEE conference on computer vision and pattern recognition. IEEE, 2007, pp. 1–8.
- [36] H. Jegou, M. Douze, and C. Schmid, "Hamming embedding and weak geometric consistency for large scale image search," in *European* conference on computer vision. Springer, 2008, pp. 304–317.
- [37] J. Philbin, O. Chum, M. Isard, J. Sivic, and A. Zisserman, "Lost in quantization: Improving particular object retrieval in large scale image

- databases," in 2008 IEEE conference on computer vision and pattern recognition. IEEE, 2008, pp. 1–8.
- [38] F. Grün, C. Rupprecht, N. Navab, and F. Tombari, "A taxonomy and library for visualizing learned features in convolutional neural networks," arXiv preprint arXiv:1606.07757, 2016.
- [39] H. Jin Kim, E. Dunn, and J.-M. Frahm, "Learned contextual feature reweighting for image geo-localization," in *Proceedings of the IEEE Conference on Computer Vision and Pattern Recognition (CVPR)*, July 2017
- [40] R. Arandjelović, P. Gronat, A. Torii, T. Pajdla, and J. Sivic, "Netvlad: Cnn architecture for weakly supervised place recognition," 2015.

#### **APPENDIX**

## A. Implementation Details

We use two base architectures which are MobileNetV2 [12] and VGG-16 [13]. The two architectures are displayed in Figure 7. The MobileNet-based method is discussed in our main content. For VGG-based method, its feature extraction branches stick out at Con3\_2, Con4\_3, and Con5\_3 respectively and their corresponding feature maps are  $\{C3_2, C4_3, C5_3\}$  having strides of  $\{4, 8, 16\}$  pixels with respect to the input image. In each feature extraction branch, the channel dimensions for  $\{C3_2, C4_3, C5_3\}$  are multiplied 1.5, 1, 0.5 times respectively and their spatial resolutions is brought back to the half of the input resolution. The obtained features from each feature extraction branch are aggregated by channel-wise concatenation. The aggregated features have channel dimensions of 1152.

Dim.	Methods on Oxford 5k									
	Ours(V)	Ours(M)	CRN	NetVLAD	SuperPoint					
4096	75.67	74.20	71.26	70.24	70.78					
2048	74.31	73.48	70.36	70.20	70.26					
1024	72.10	71.78	68.20	67.88	68.03					
512	70.92	69.47	66.24	65.99	66.10					
256	67.66	66.88	63.95	63.09	63.14					
128	63.48	62.20	57.21	57.10	57.18					
64	55.48	54.20	50.26	49.65	49.80					
32	48.10	47.46	43.72	43.00	43.30					
16	38.24	37.26	33.20	32.68	32.96					
Dim.	Methods on Paris 6k									
Dilli.	Ours(V)	Ours(M)	CRN	NetVLAD	SuperPoint					
4096	82.21	81.57	76.45	76.23	76.40					
2048	81.10	80.82	75.25	76.10	76.20					
1024	79.88	79.34	75.47	75.27	75.31					
512	77.78	77.45	74.08	73.68	73.93					
256	75.03	75.00	72.88	72.53	72.83					
128	71.20	70.67	67.58	66.65	67.42					
64	67.21	64.39	61.92	60.67	61.32					
32	59.62	57.43	52.40	51.89	52.20					
16	52.02	49.19	44.23	43.67	44.10					
Dim.	Methods on Holidays									
Dini.	Ours(V)	Ours(M)	CRN	NetVLAD	SuperPoint					
4096	86.89	86.57	85.42	84.82	85.10					
2048	86.73	86.45	85.33	84.80	85.23					
1024	86.62	86.20	84.89	84.62	84.78					
512	85.69	85.10	84.21	83.99	84.10					
256	84.71	84.01	83.19	82.67	82.92					
128	81.46	80.79	79.75	79.20	79.68					
64	77.12	76.34	74.67	74.32	74.50					
32	69.78	68.32	65.40	64.78	65.25					
16	59.78	59.20	54.56	53.78	54.10					

TABLE V. Comparison with state-of-the-art methods for compact image representations for varying dimentionality on image retrieval tasks. Ours(V) has VGG backbone and ours(M) has MobileNet backbone.

In training, we use the margin m = 0.1, 30 epochs, learning rate 0.001 (for MobileNet-based method) or 0.0001 (for VGG-based method), which is halved in every 5 epochs, momentum 0.9, weight decay 0.001, and batch size of 4 triplets. Following the implementation from [39], we also exploit standard data augmentation in training, such as motion blur, random Gaussian noise, brightness changes to improve the robustness of our methods to illumination

variations and viewpoint changes. Since this implementation allow us achieve desired training results but convergence generally occurs faster than the designated training length, we choose the saved models which yield the best recall@5 on the validation set is used for testing.

In preparing for the training dataset, we use all the potential positive images (images within 10 meters to the query input), and then we perform randomized negative data mining for the negative images (images are than 25 meters to the query input). We use the same data mining technique from [40] in order to increase the training efficiency and effectiveness.

#### B. Additional Results and Discussions

**Results of ablation study.** We display the results for the MobileNet-based methods (Figure 8a). Method a is the strong baseline while method b and c are two variants with one extra feature extraction branch at lower- and mid-level semantics respectively. Method d is the proposed method. We can see that adding the feature extraction branch can improve the localization performance on different benchmarks.

Large-scale localization benchmark results. Figure 8b displays the comparison of Recalls at N top retrievals of state-of-the-art methods on the Pitts250k-test, TokyoTM-val, Tokyo 24/7and Sf-0 datasets. Our methods outperform the existing leading methods on all benchmarks. Particularly, our methods lead other methods by a significant margin where the retrieval number is low.

Qualitative analysis also demonstrates that, compared to other methods which may include confusing features from pedestrians, vegetation, or vehicles which are hard for keypoint repeatability, our method focuses on discriminative details on building for localization prediction (Figure 9).

Qualitative results on Patches dataset. The results indicate that our MobileNet and VGG-based architectures outperform the strong baseline as they can generate denser keypoint features for effective matching. Our methods also have better feature repeatability than the baseline (Figure 10).

**Image retrieval task results.** We further evaluate our methods on each image retrieval task by varying the dimenstionality. Our methods outperform state-of-the-art methods for the compact image representations on each dimenstionality (as shown Table V).

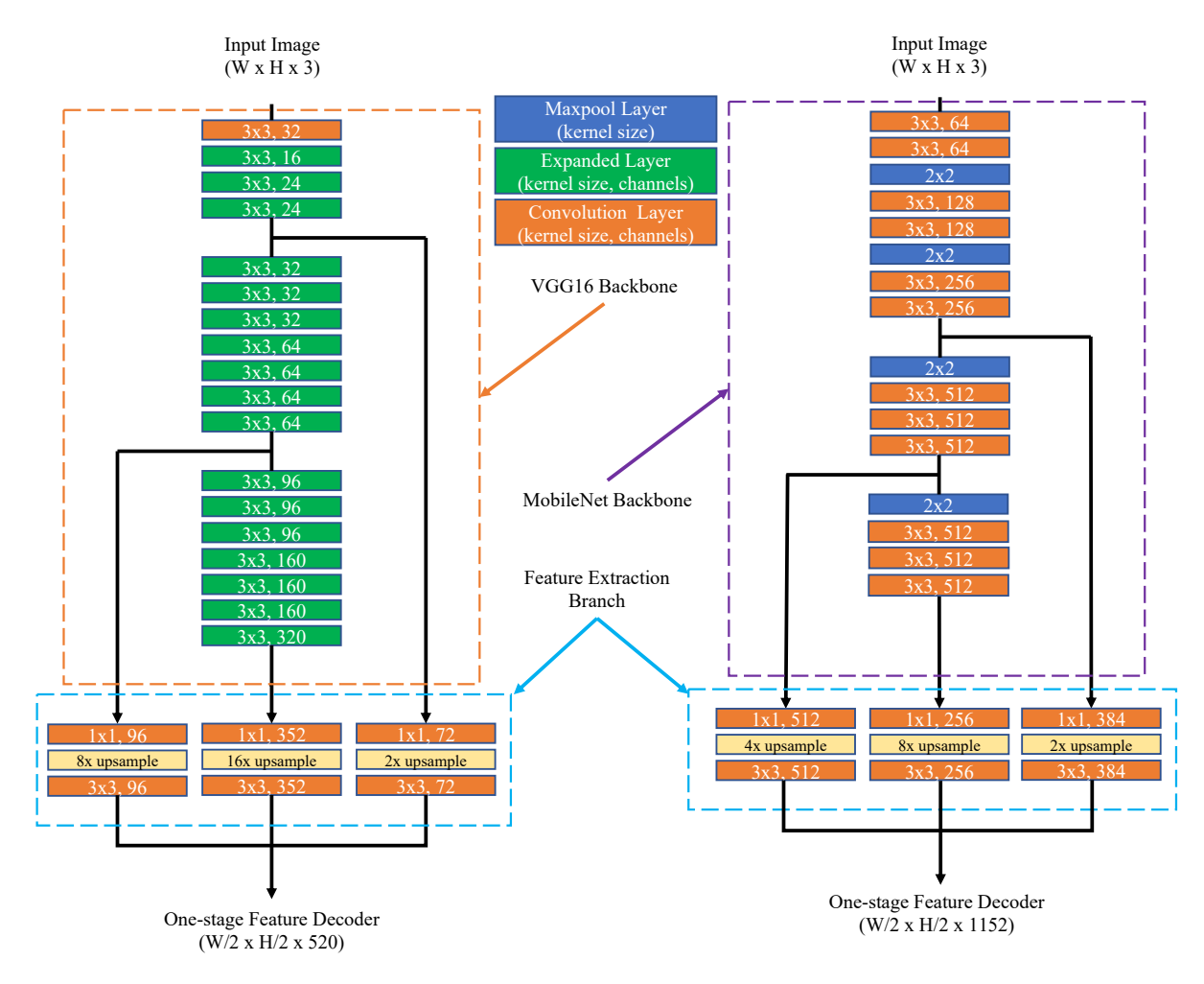


Fig. 7. Architectures of the proposed method.

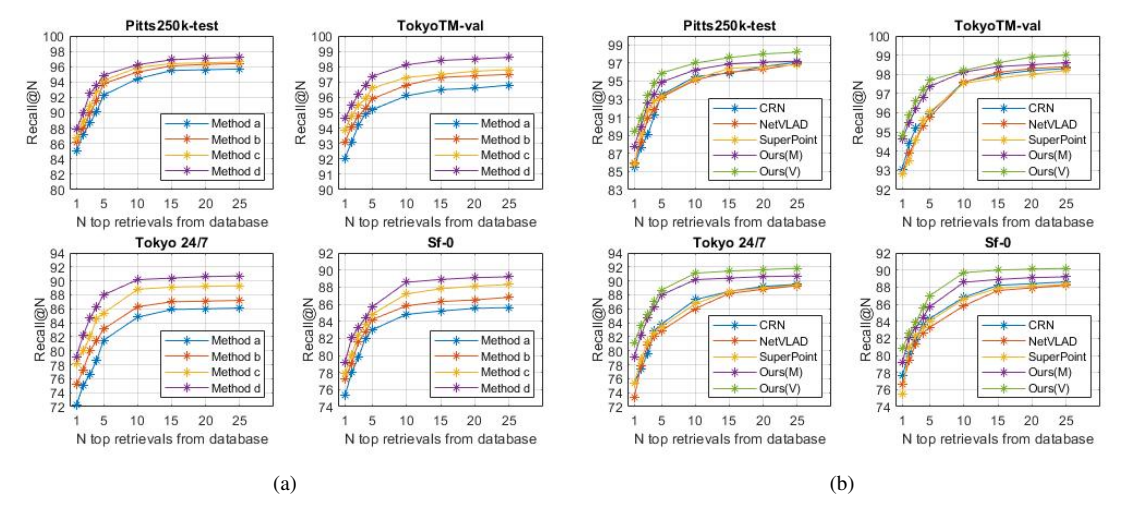


Fig. 8. Additional results. (a) Ablation results of recalls at N top retrievals with all MobileNet-based methods. (b) Comparison of recalls at N top retrievals with state-of-the-art methods. Ours(V) has VGG backbone and ours(M) has MobileNet backbone.

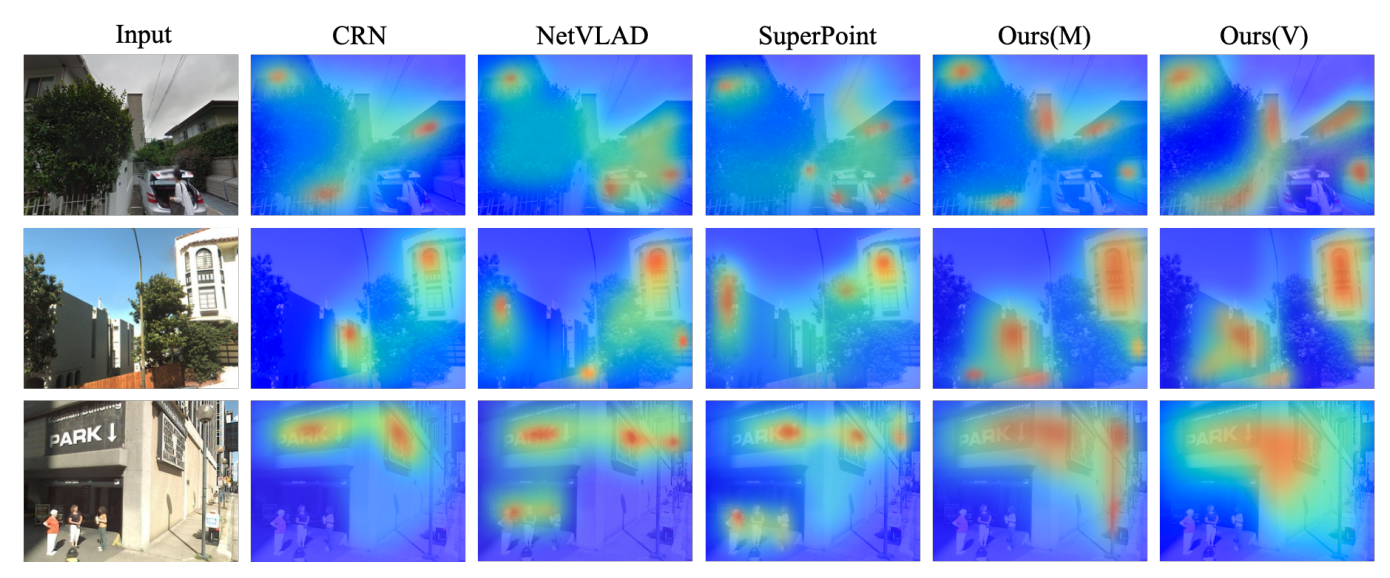


Fig. 9. Comparison of feature emphasis of each method. M and V in ours mean MobileNet and VGG backbone respectively.

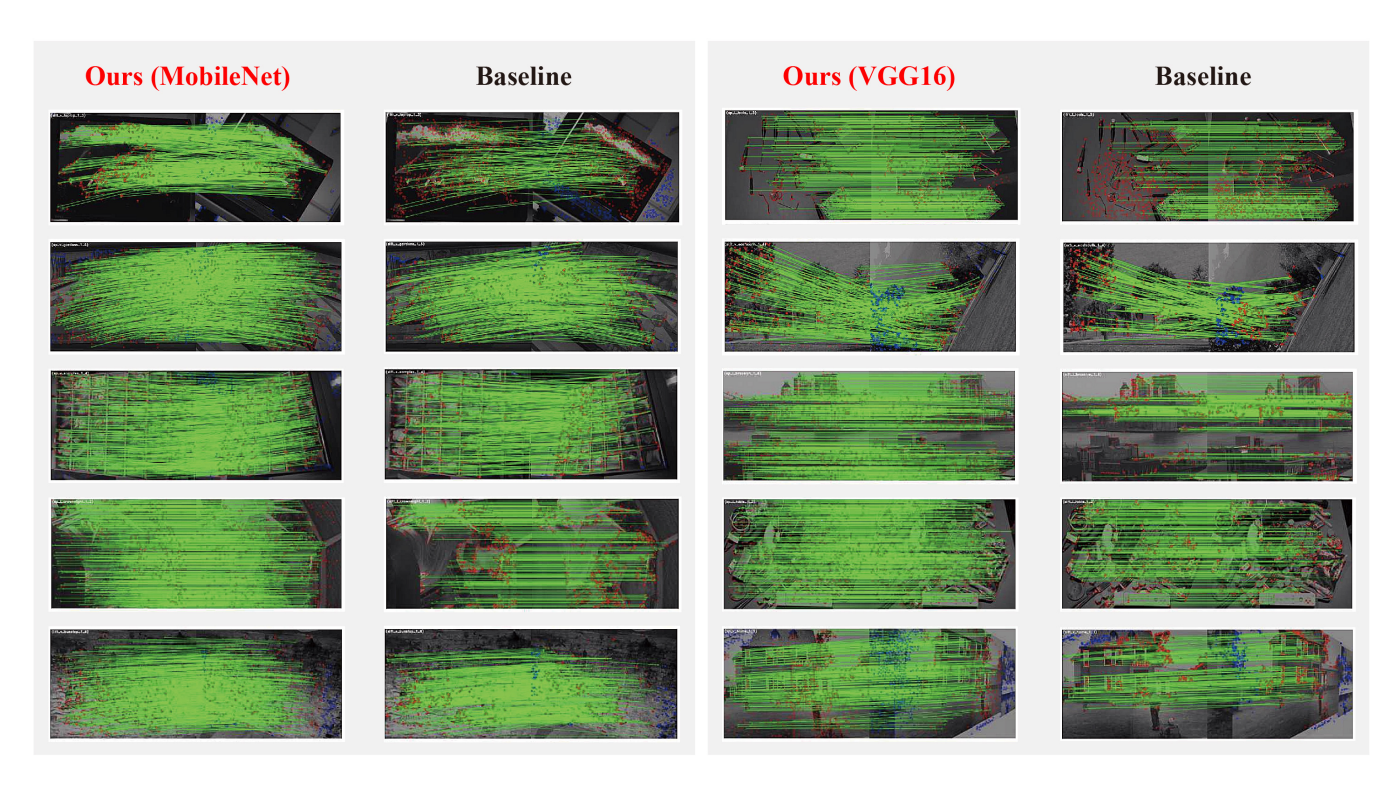


Fig. 10. Qualitative examples on the HPatches dataset. The green lines indicate all correct correspondences which are repeatable. DenserNet can produce denser and more correct matches compared to the baseline method. Red dots are mismatched points and blue dots are not visible to the shared viewpoint region of the image pairs.